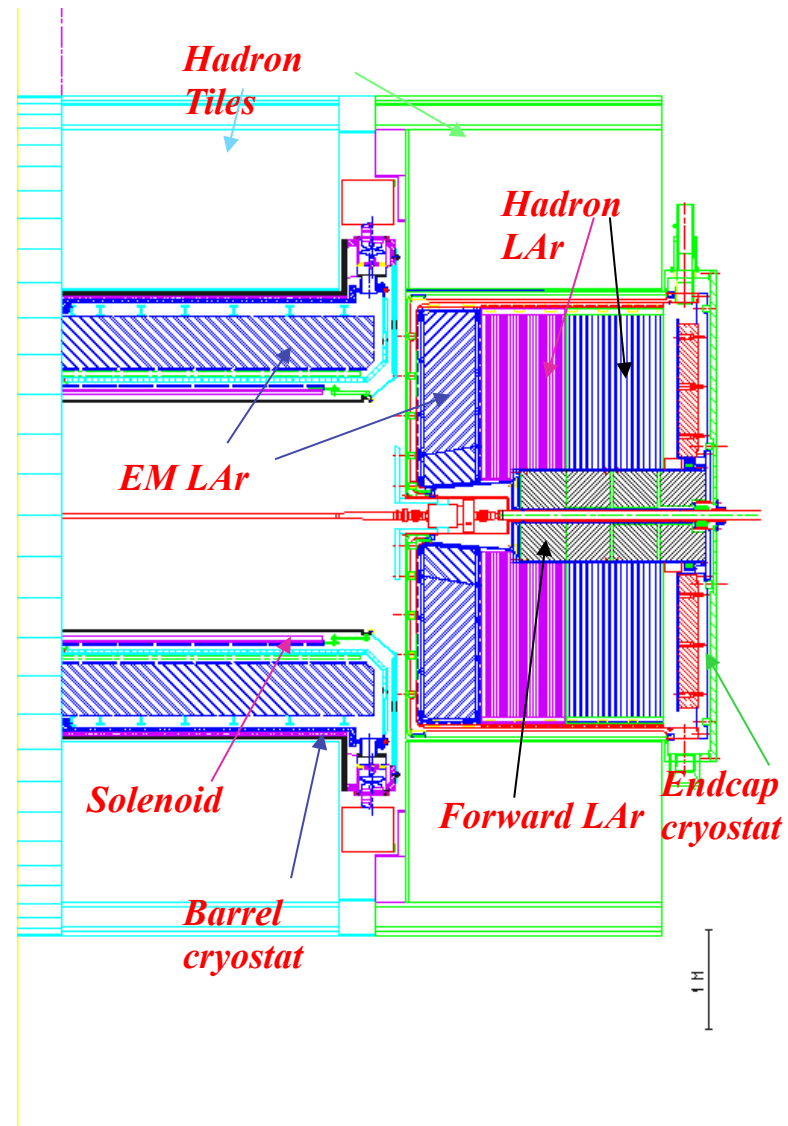
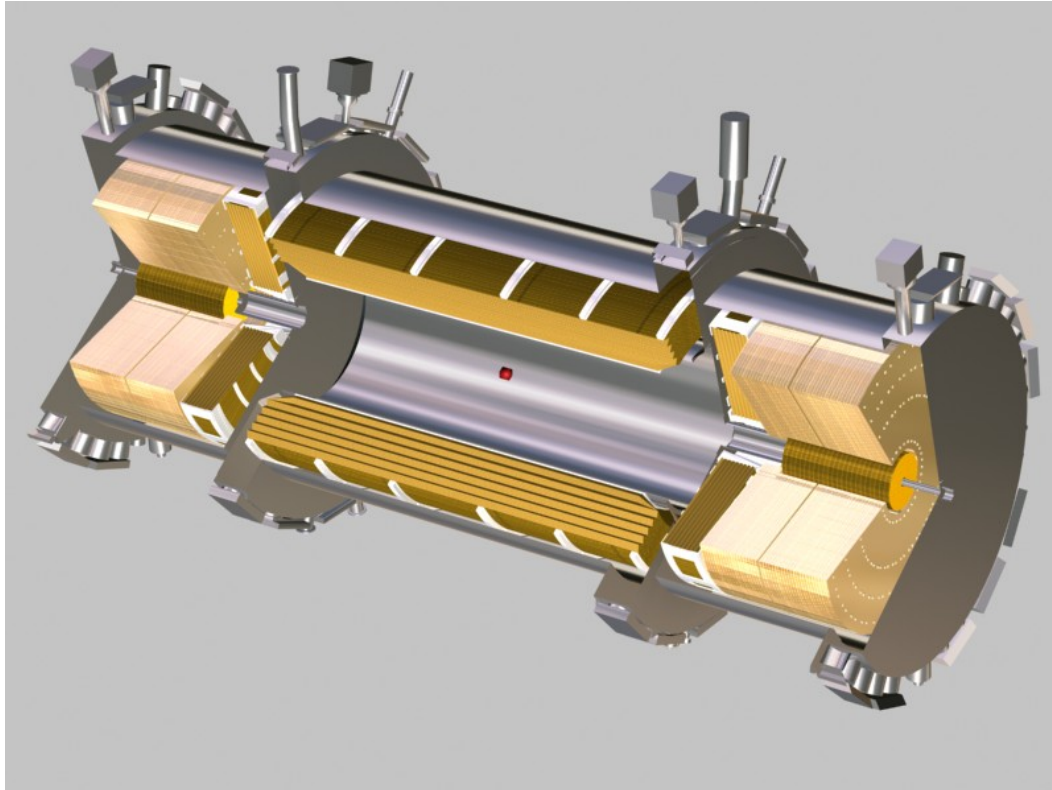


Calorimetry

The LAr calorimetry (pre-samplers, EM, hadronic end-caps, and forward calorimeters)



Calorimetry

(based on Bartoletto lectures at CERN)

Particle detection via total absorption

- almost all energy transformed into heat -> calorimeter

Destructive measurement

- Electromagnetic showers

- Hadronic interactions

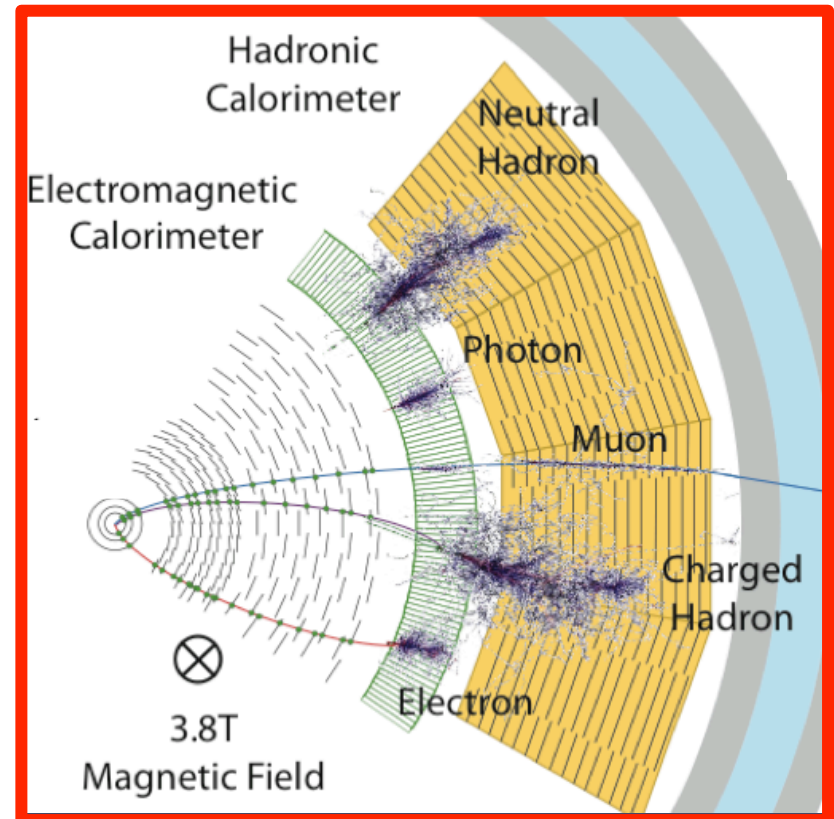
Essential for detection of neutral particles

Can identify muons via minimum ionization

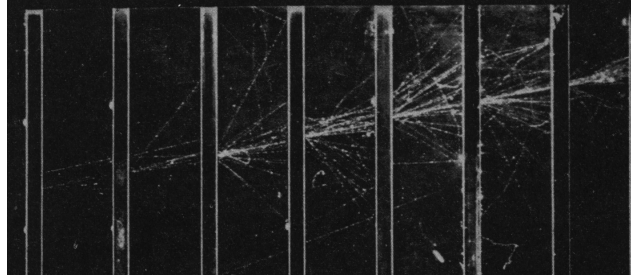
Hermetic calorimeter can detect

ME - missing energy, difference between collision energy and detected energy

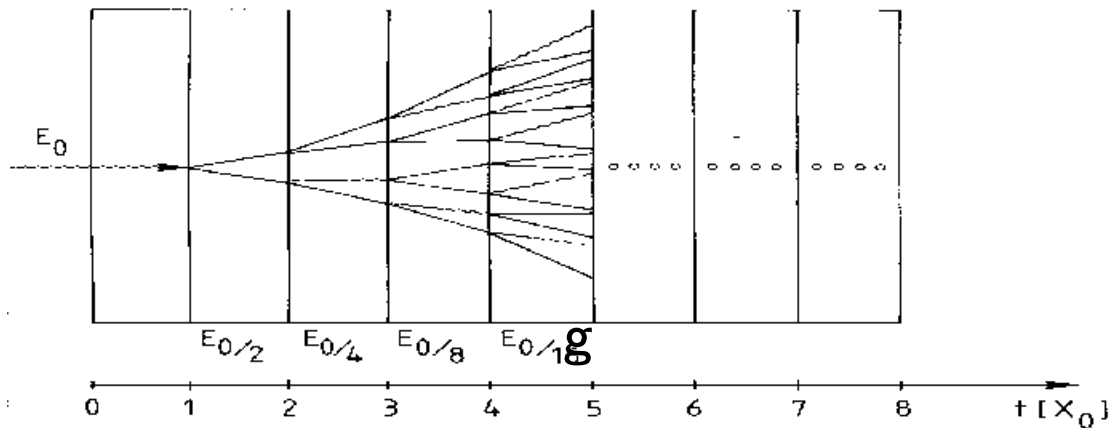
ME – can be due to neutrinos or new neutral weakly interacting particles



Electromagnetic cascades (showers)



Electron shower
in a cloud
chamber with
lead absorbers



Consider only **Bremsstrahlung**
and **pair production**.

Assume: $X_0 = l_{\text{pair}}$

$$N(t) = 2^t \quad E(t) / \text{particle} = E_0 \cdot 2^{-t}$$

Process continues until $E(t) < E_c$

$$t_{\text{max}} = \frac{\ln E_0 / E_c}{\ln 2}$$

$$N^{\text{total}} = \sum_{t=0}^{t_{\text{max}}} 2^t = 2^{(t_{\text{max}}+1)} - 1 \approx 2 \cdot 2^{t_{\text{max}}} = 2 \frac{E_0}{E_c}$$

After $t = t_{\text{max}}$ the dominating processes are **ionization**, **Compton effect** and **photo effect** + **absorption**.

Electromagnetic cascades

Longitudinal shower development: $\frac{dE}{dt} \propto t^\alpha e^{-t}$

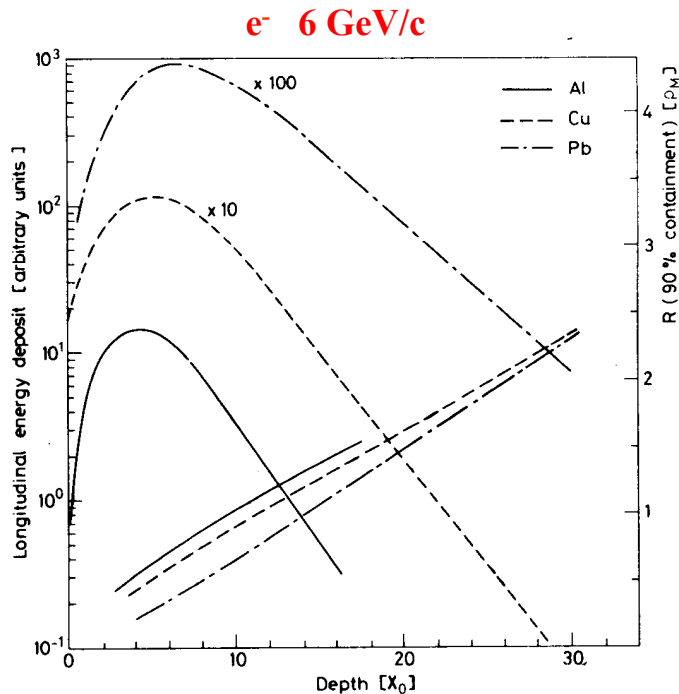
Shower maximum at $t_{\max} = \ln \frac{E_0}{E_c} \frac{1}{\ln 2}$

Size of a calorimeter grows logarithmically with E_0

95% containment $t_{95\%} \approx t_{\max} + 0.08Z + 9.6$

Transverse shower development: 95% of the shower cone is located in a cylinder with radius $2 R_M$ **Moliere radius**

$$R_M = \frac{21 \text{ MeV}}{E_c} X_0 \quad [g/cm^2]$$

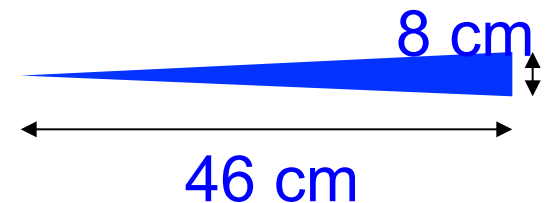


Longitudinal and transverse development scale with X_0 , R_M

Example: $E_0 = 100$ GeV in lead glass

$E_c = 11.8$ MeV $t_{\max} \approx 13$, $t_{95\%} \approx 23$

$X_0 \approx 2$ cm, $R_M = 1.8 \cdot X_0 \approx 3.6$ cm



Electromagnetic shower

- Dominant processes at high energies ($E > \text{few MeV}$):

- Photons: Pair production

$$\sigma_{pair} \approx \frac{7}{9} \left(4\alpha r_e^2 Z^2 \ln \frac{183}{Z^{1/3}} \right) = \frac{7}{9} \frac{A}{N_A X_0}$$

$$I(x) = I_0 e^{-\mu x} \quad \mu = \frac{7}{9} \frac{\rho}{X_0}$$

μ = attenuation coefficient

X_0 = radiation length in [cm] or [g/cm²]

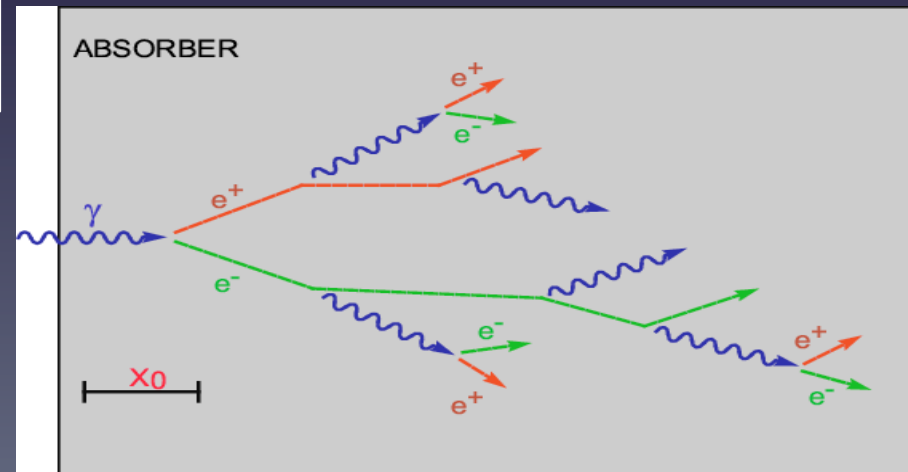
$$X_0 = \frac{A}{4\pi N_A Z^2 r_e^2 \ln \frac{183}{Z^{1/3}}}$$

- Electrons: Bremsstrahlung

$$\frac{dE}{dx} = 4\alpha N_A \frac{Z^2}{A} r_e^2 E \ln \frac{183}{Z^{1/3}} = \frac{E}{X_0}$$

$$E = E_0 e^{-x/X_0}$$

After traversing $x=X_0$ the electron has only $1/e=37\%$ of its initial energy



Analytic shower Model

Simplified model [Heitler]: shower development governed by X_0

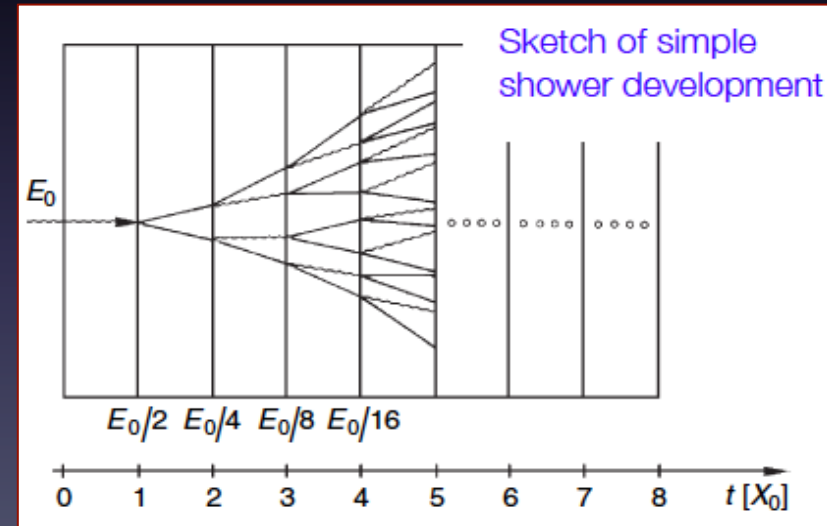
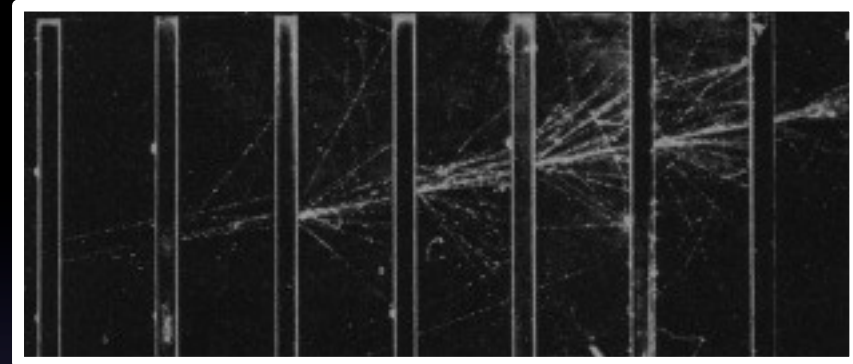
- e^- loses $[1 - 1/e] = 63\%$ of energy in 1 X_0 (Brems.)
- the mean free path of a γ is $9/7 X_0$ (pair prod.)

Assume:

- $E > E_c$: no energy loss by ionization/excitation

Simple shower model:

- $N(t) = 2^t$ particles after $t = x/X_0$ each with energy $E(t) = E_0/2^t$
- Stops if $E(t) < E_c = E_0 2^{t_{\max}}$
- Location of shower maximum at



$$t_{\max} = \frac{\ln(E / E_c)}{\ln 2} \approx \ln \frac{E}{E_c}$$

$$N_{\max} = 2^{t_{\max}} = \frac{E_0}{E_c}$$

Different shower shape for electron and photon

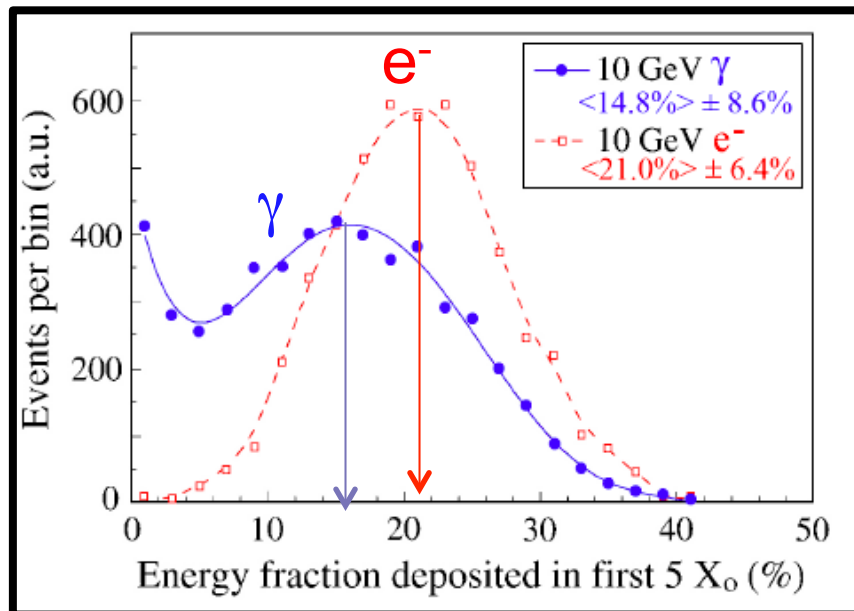
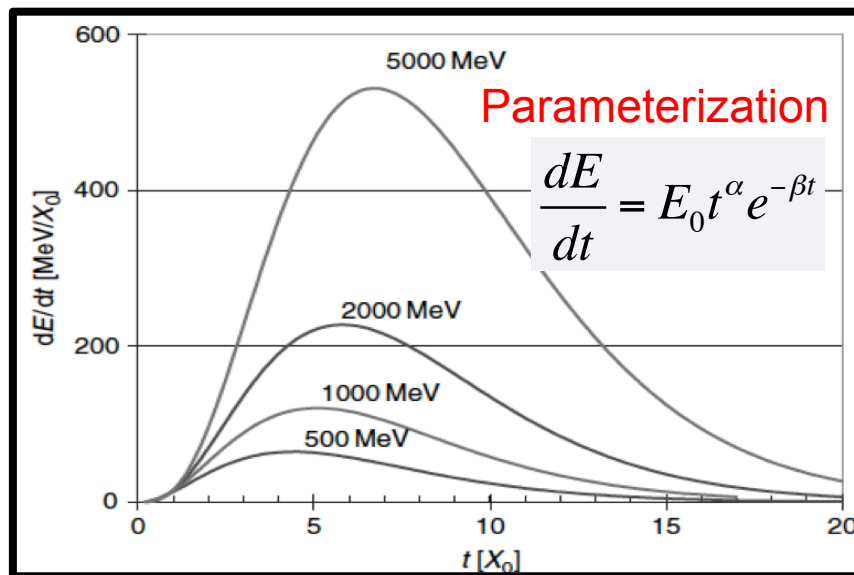
- due to difference between brehmsstrahlung and conversion

X_0 – radiation length

$$t_{\max} = \ln\left(\frac{E_0}{E_c}\right) + C_{ey}$$

$C_{ey} = -0.5$ for photons

$C_{ey} = -1.0$ for electrons



Longitudinal shower containment

- Since $t_{\max} \approx \ln(E) \rightarrow$ calorimeter thickness must increase as $\ln(E)$
- After shower max showering will stop in $\approx 1X_0$
- To absorb 95% of photons after shower max $\approx 9X_0$ of material are needed
- The energy leakage is mainly due to photons
- A useful expression to indicate 95% shower containment

A useful expression to indicate 95% shower containment is:

$$L(95\%) = t_{\max} + 0.08 Z + 9.6 [X_0]$$

$$\begin{array}{llll} E_C \approx 10 \text{ MeV} & E_0 = 1 \text{ GeV} & \Rightarrow t_{\max} = \ln 100 / \ln 2 \approx 6.6 & N_{\max} = 100 \\ & E_0 = 100 \text{ GeV} & \Rightarrow t_{\max} = \ln 10,000 / \ln 2 \approx 9.9 & N_{\max} = 10,000 \end{array}$$

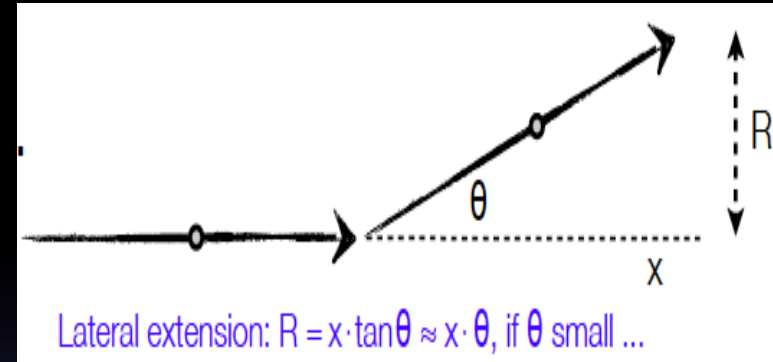
	Scint.	LAr	Fe	Pb	W
$X_0(\text{cm})$	34	14	1.76	0.56	0.35

Lateral development of EM shower

Opening angle:

- bremsstrahlung and pair production

$$\langle \theta^2 \rangle \approx \frac{m_e c^2}{E_e} \frac{\sigma^2}{\lambda} -$$



- multiple coulomb scattering [Molière theory]

$$\langle \theta \rangle = \frac{E_s}{E_e} \sqrt{\frac{x}{X_0}} \quad \text{where} \quad E_s = \sqrt{\frac{4\pi}{\alpha}} (m_e c^2) = 21.2 \text{ MeV}$$

- Main contribution from low energy e^- as $\langle \theta \rangle \sim 1/E_e$, i.e. for e^- with $E < E_c$

Molière Radius

$$R_M = \frac{E_s}{E_c} X_0 \approx \frac{21.2 \text{ MeV}}{E_c} X_0$$

- Assuming the approximate range of electrons to be X_0 yields $\langle \theta \rangle \approx 21.2 \text{ MeV}/E_e \rightarrow$ lateral extension: $R = \langle \theta \rangle X$

Lateral development of EM shower

Inner part is due to Coulomb's scattering of electron and positron

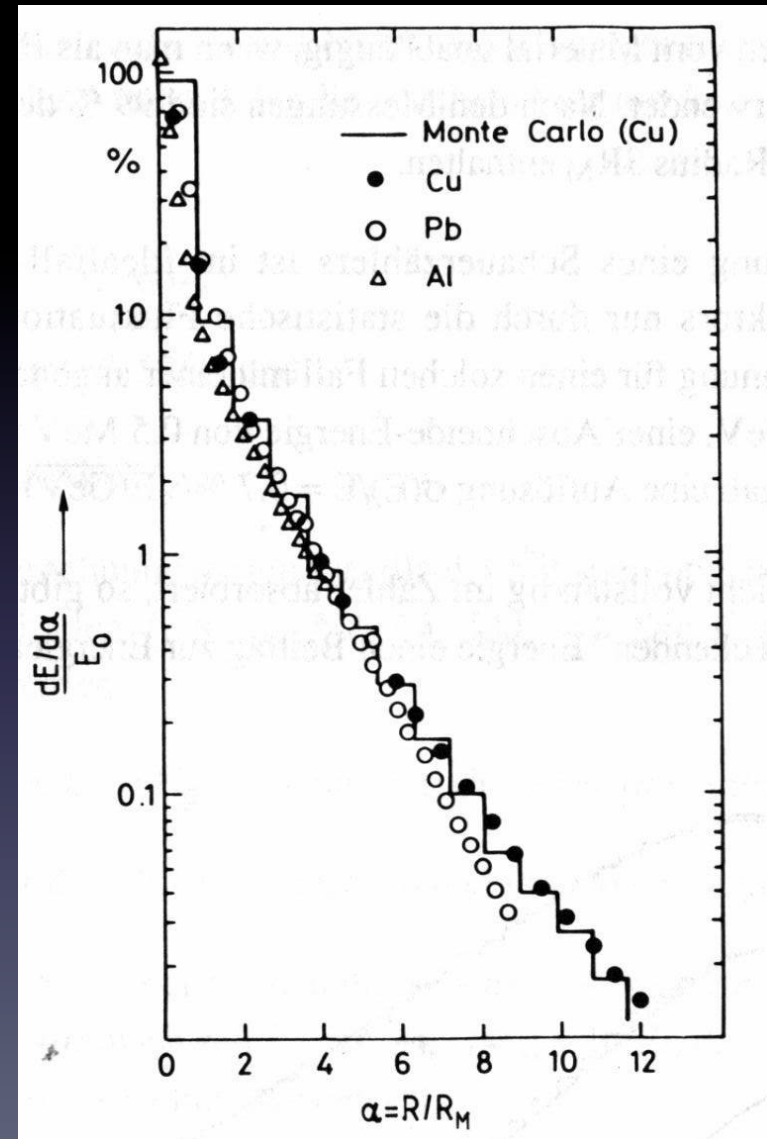
Outer part is due to low energy γ produced in Compton's scattering, photo-electric effect etc.

- Predominant part after shower max especially in high Z absorbers

$$\frac{dE}{dr} = \alpha e^{-r/R_M} + \beta e^{-r/\lambda_{\min}}$$

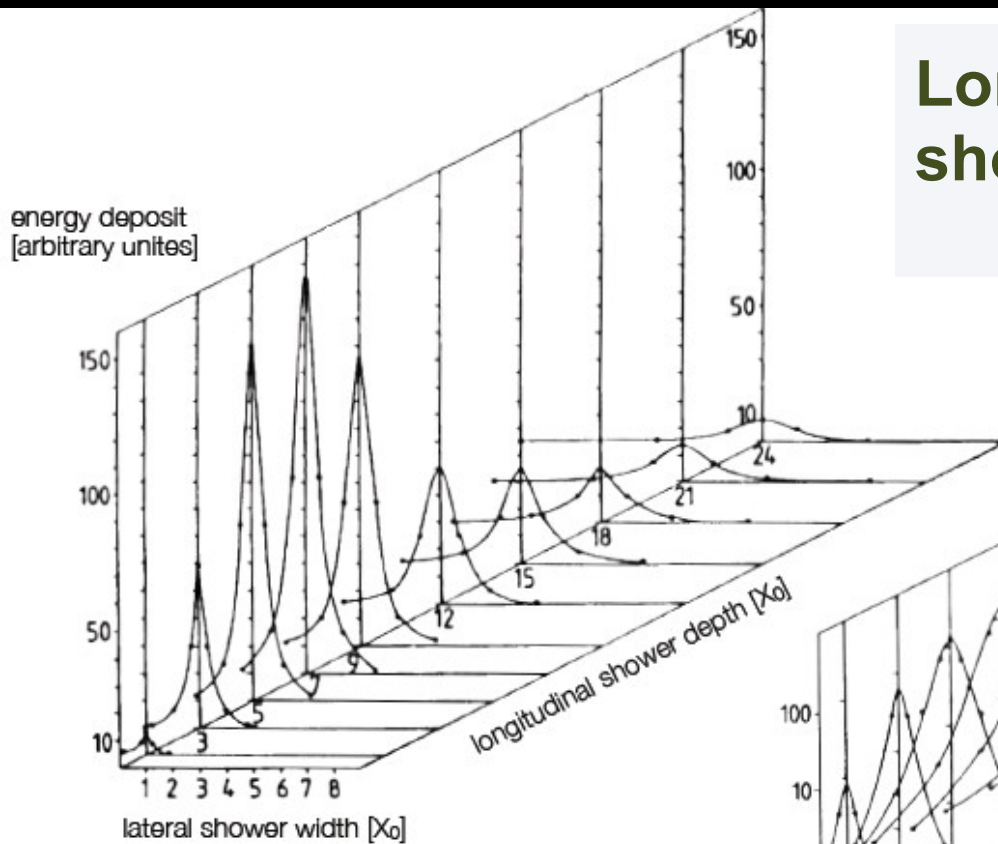
The shower gets wider at larger depth

An infinite cylinder of radius $2R_M$ contains 95% of the shower

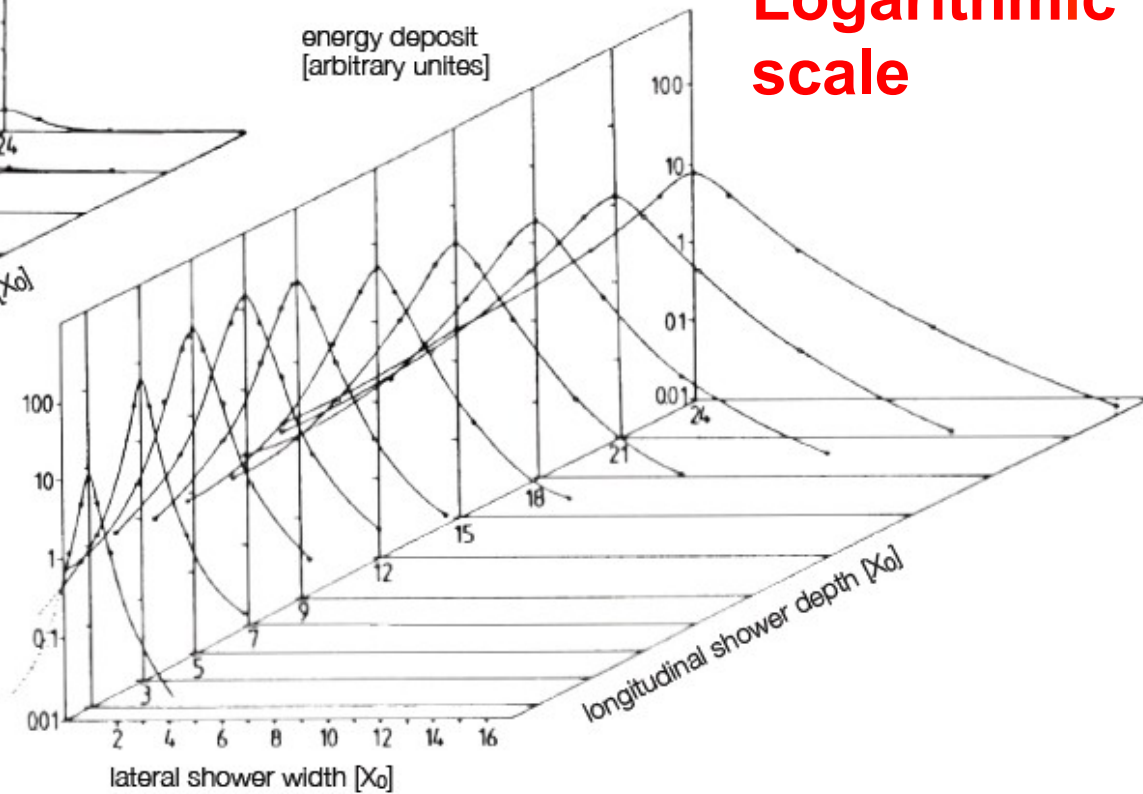


3D EM Shower development

Longitudinal and transfer EM shower profile of 6 GeV e^- in Pb

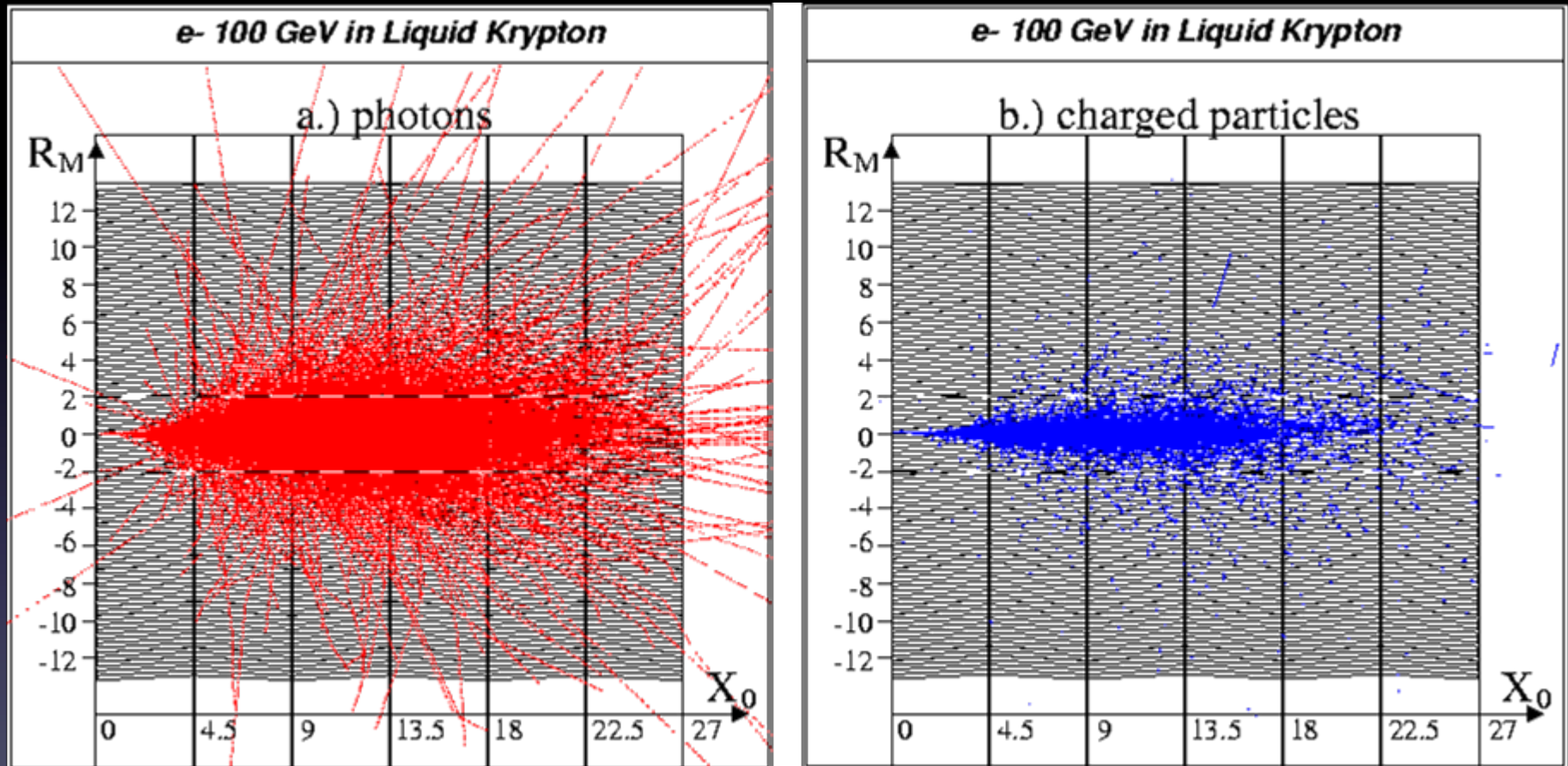


Linear scale



Logarithmic scale

EM shower development in liquid krypton ($Z=36$, $A=84$)



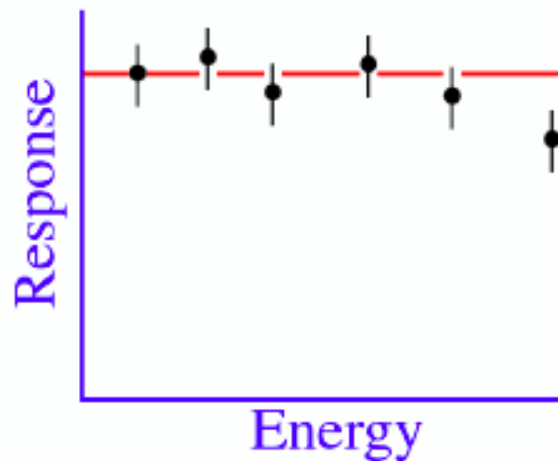
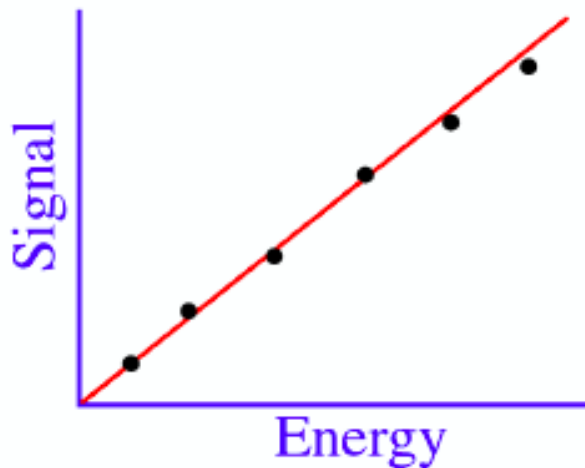
GEANT simulation of a 100 GeV electron shower in the NA48 liquid Krypton calorimeter (D.Schinzel)

Discussion: Explain why they are different

Energy Measurement

How we determine the energy of a particle from the shower?

- Detector response → Linearity
 - The average calorimeter signal vs. the energy of the particle
 - Homogenous and sampling calorimeters
 - Compensation (for hadronic showers)
- Detector resolution → Fluctuations
 - Event to event variations of the signal
 - What limits the accuracy at different energies?



Signal per unit of deposited energy

EM calorimeters are linear
Hadronic calorimeters are not linear

Sources of Non Linearity

- Instrumental effects
 - saturation of gas detectors, scintillators, photo-detectors, electronics
- Response varies with something that varies with energy
- Examples:
 - Deposited energy “counts” differently, depending on depth and depth increases with energy
- Leakage (increases with energy)

Signal linearity for electromagnetic showers

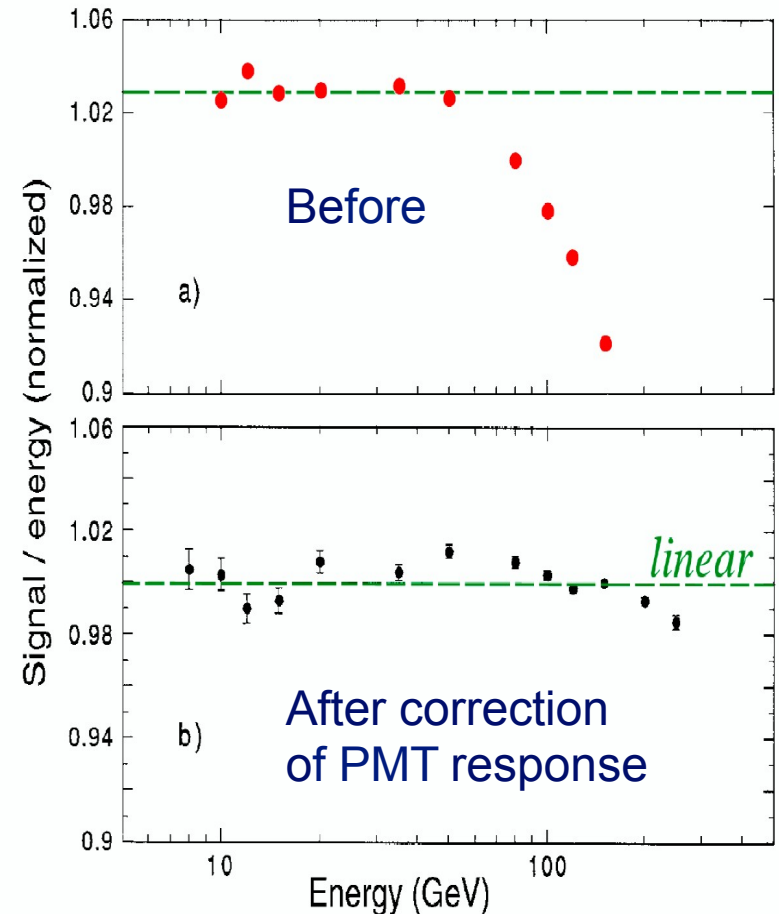


FIG. 3.1. The em calorimeter response as a function of energy, measured with the QFCAL calorimeter, before (a) and after (b) precautions were taken against PMT saturation effects. Data from [Akc 97].

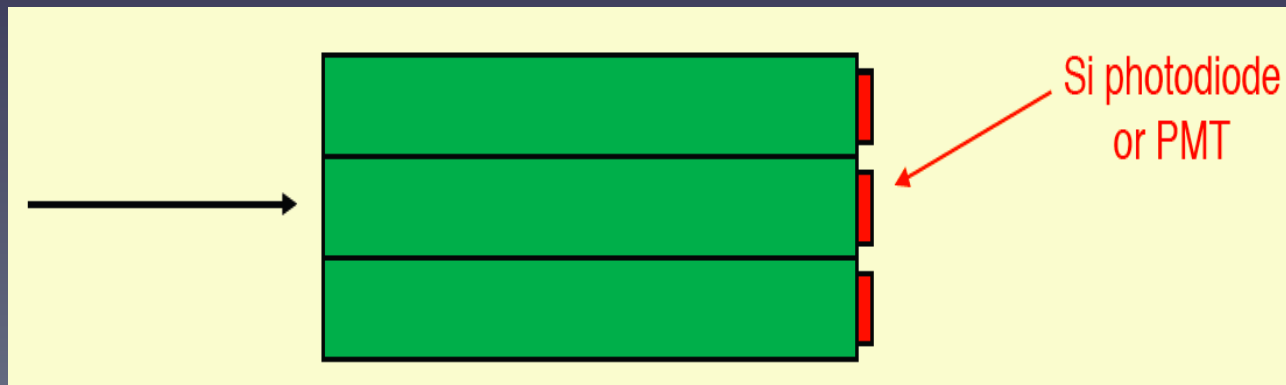
EM Calorimeter configurations

Total absorption

- Electrons and photons stop in calorimeter
- Scintillation proportional to energy of electron
- Usually non-organic scintillator (BGO, PbWO_4, \dots) or liquid Xe
- Advantage: Excellent energy resolution
 - see all charged particles in the shower (but for shower leakage) best statistical precision
 - > uniform response, good linearity
- Disadvantages:
 - cost and limited segmentation

If W is the mean energy required to produce a signal (eg an e-ion pair in a noble liquid or a 'visible' photon in a crystal)

$$\frac{\sigma_E}{E} = \frac{1}{\sqrt{n}} = \frac{1}{\sqrt{E/W}}$$



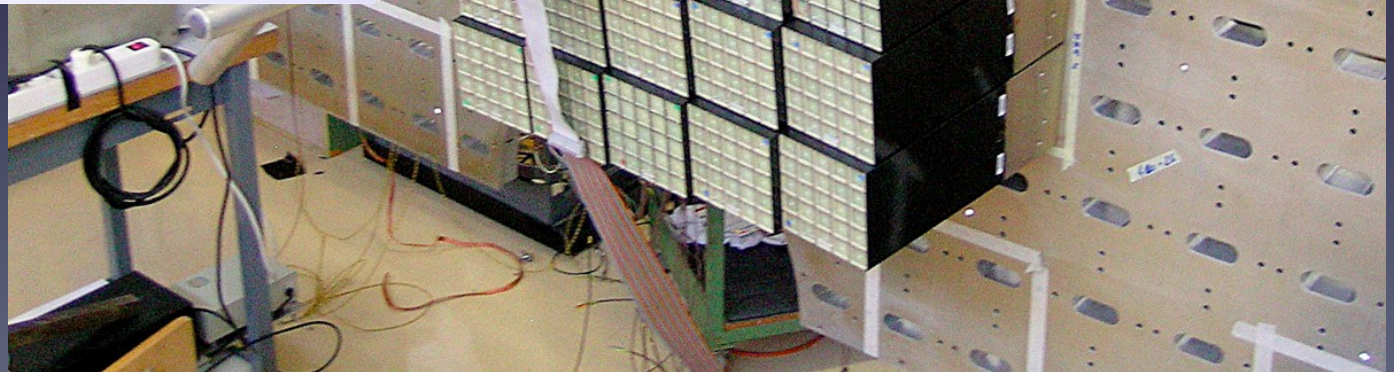
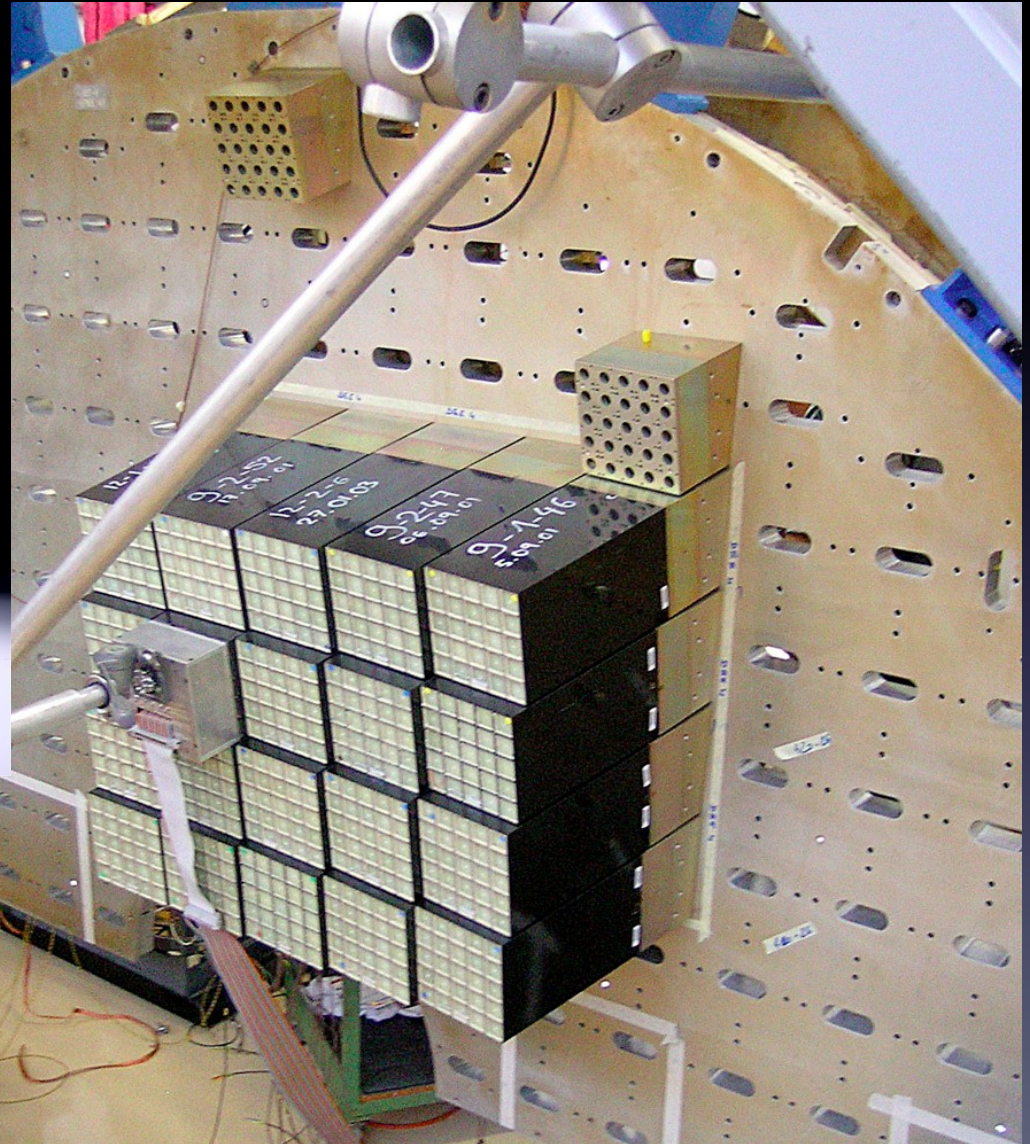
Homogenous calorimeters

Barrel: 62K $2.2 \times 2.2 \times 23$ cm³ crystals

Endcap: 15K $3 \times 3 \times 22$ cm³ crystals

PbWO₄ radiation hard crystals

1% resolution at 30 GeV



EM Calorimeter configurations

Sampling Calorimeter

- One material to induce showering (high Z)
- Another to detect particles (typically by counting number of charged tracks)
- Many layers sandwiched together
- Resolution $\propto E^{-1/2}$

Advantages

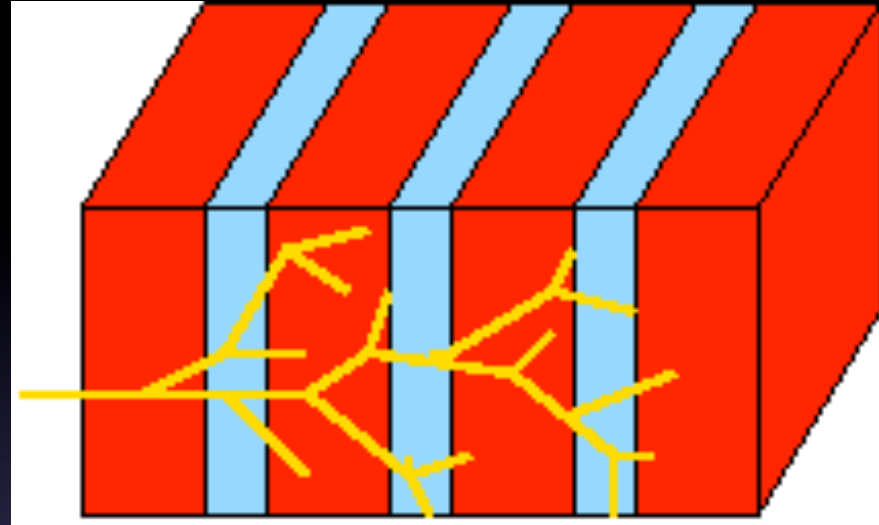
- Depth segmentation
- Spatial segmentation

Disadvantages:

- Only part of shower seen, less precise

Examples

- ATLAS ECAL
- Most HCALs

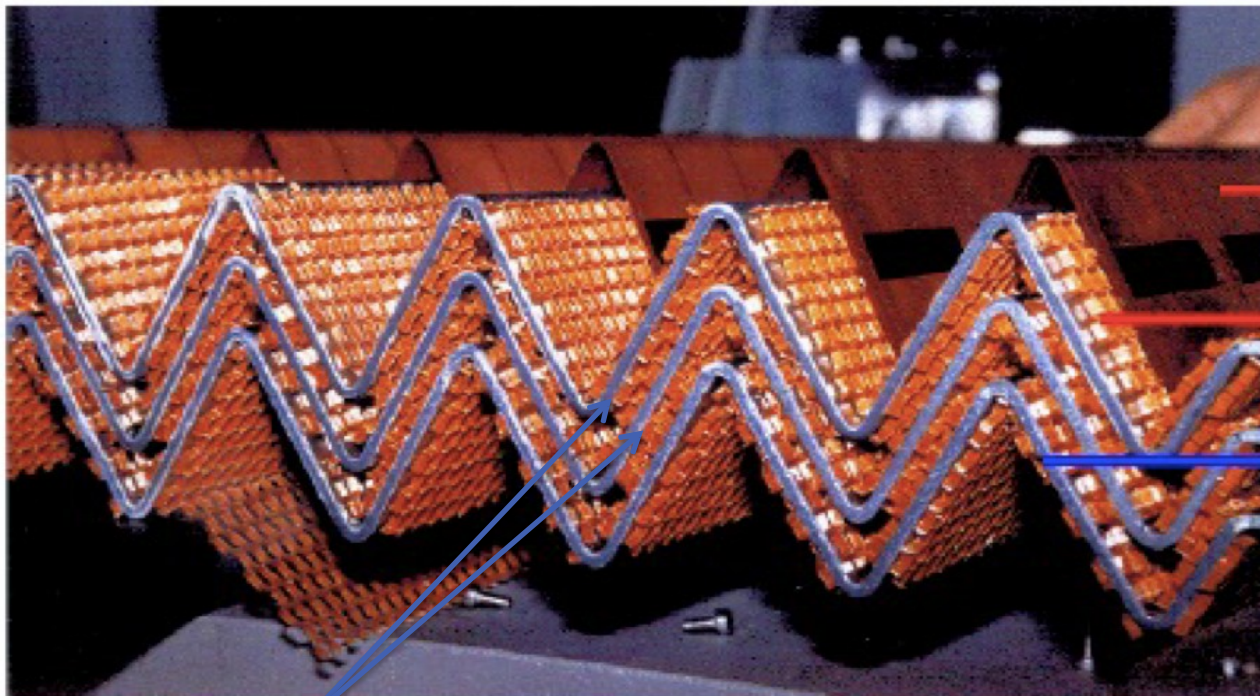
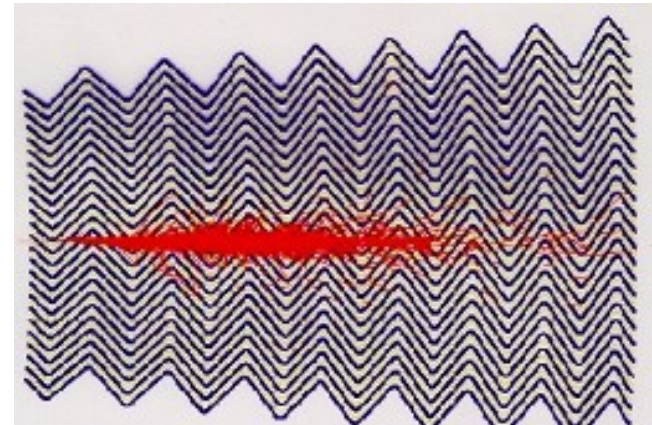


Sampling fraction

$$f_{\text{sampling}} = \frac{E_{\text{visible}}}{E_{\text{deposited}}}$$

ATLAS Liquid Argon ECAL

~220,000 individual readout channels
multiplexed into towers for trigger

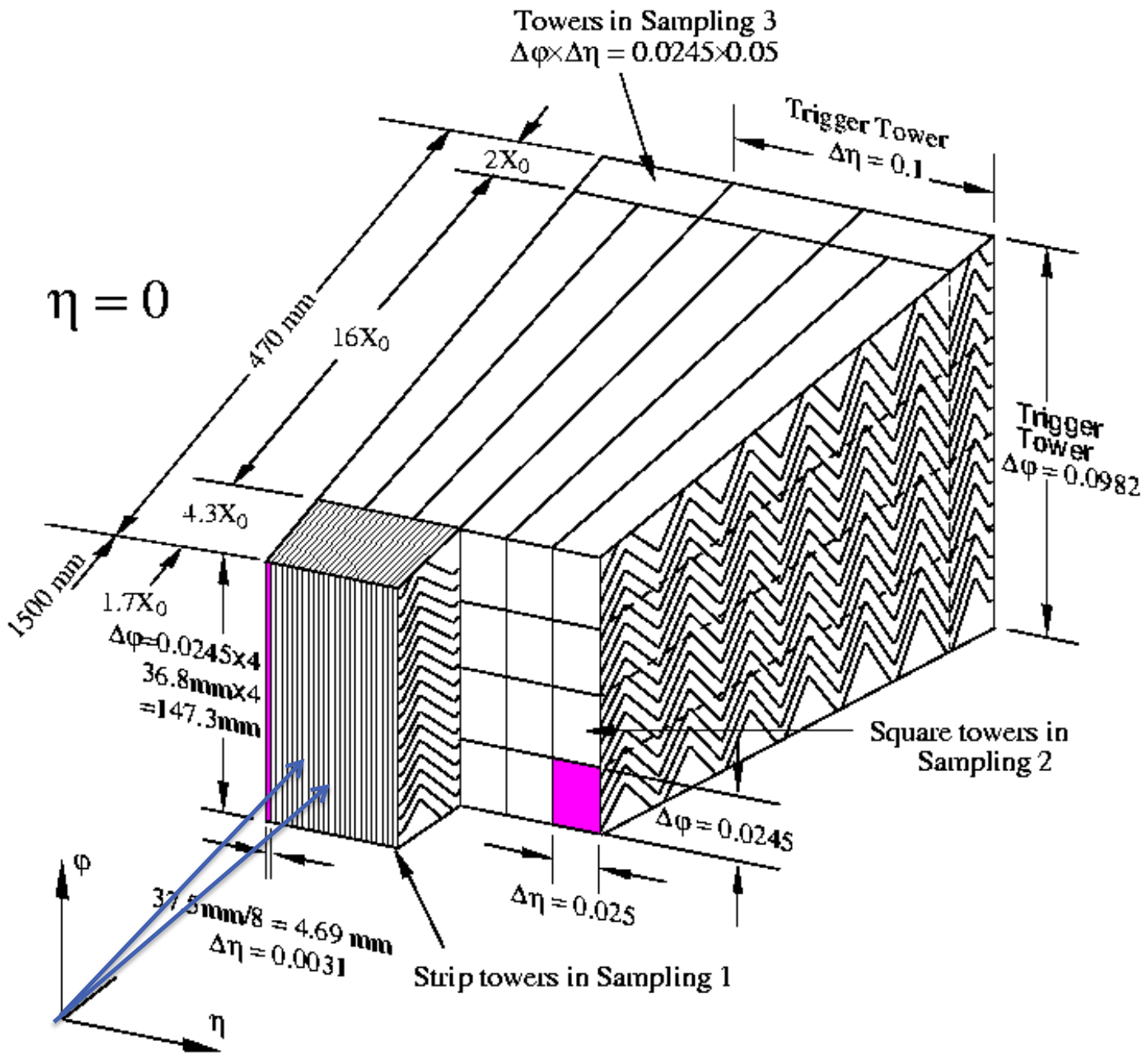


Cu electrodes at +HV

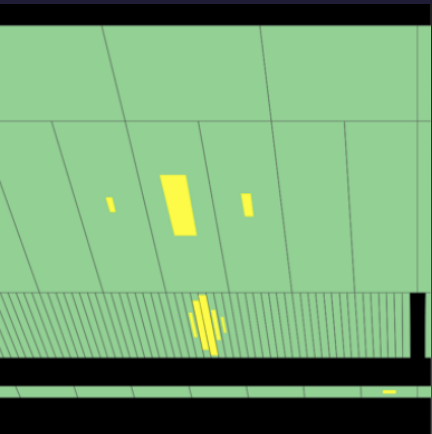
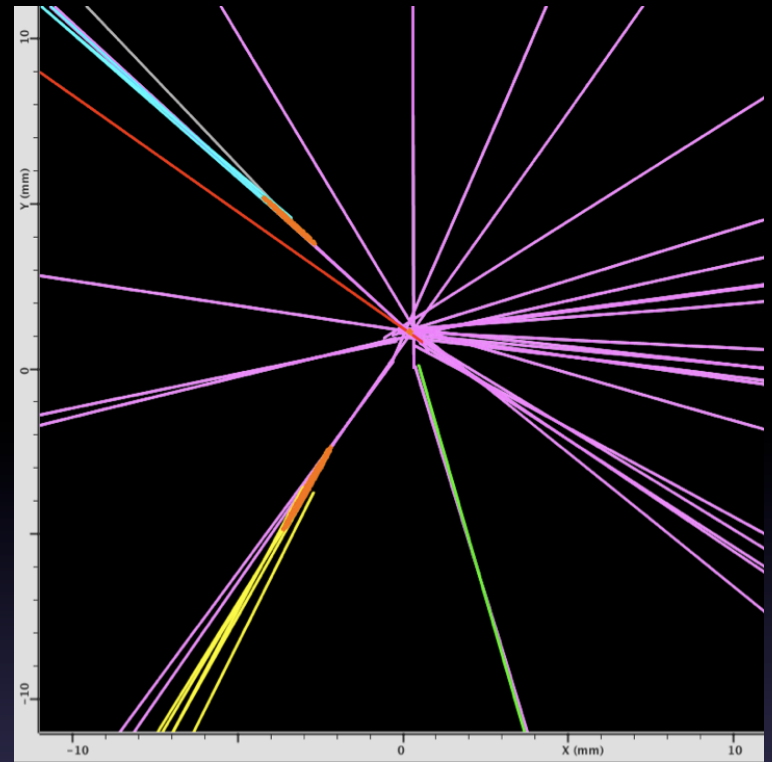
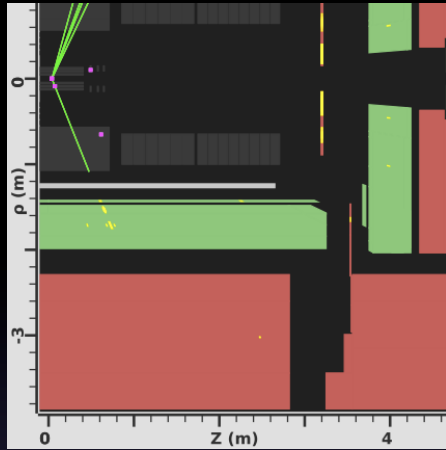
Spacers define LAr gap
 2×2 mm

2 mm Pb absorber
clad in stainless steel.

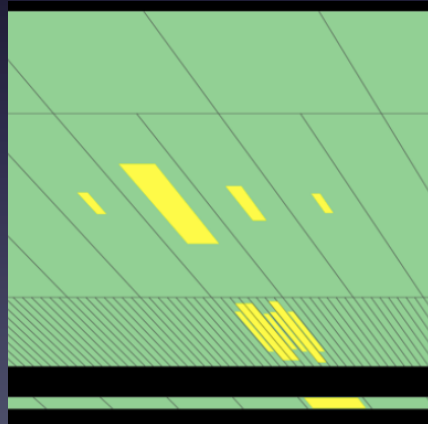
hexel spacers



Signatures

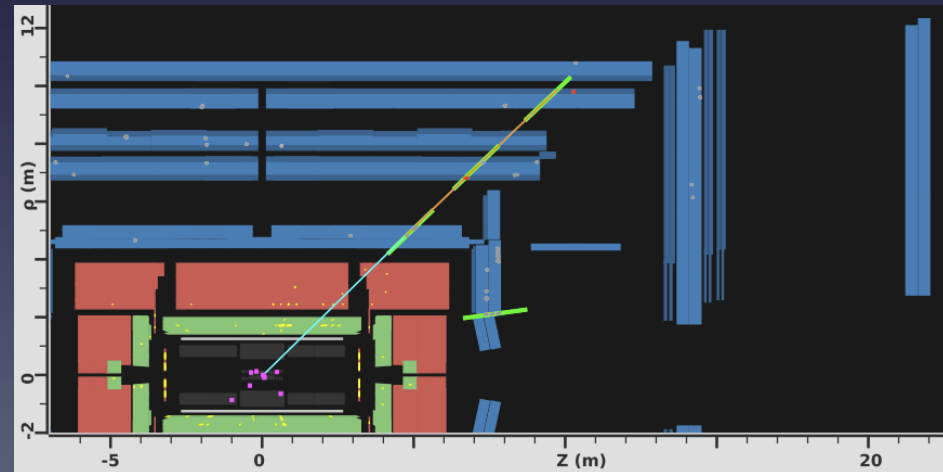


photon



π^0

muon



Energy resolution

■ Ideally, if all shower particles counted

$$E \propto N \quad \sigma_E \approx \sqrt{N} \approx \sqrt{E}$$

■ In practice

$$\sigma_E = a\sqrt{E} \oplus bE \oplus c \quad \frac{\sigma_E}{E} = \frac{a}{\sqrt{E}} \oplus b \oplus \frac{c}{E}$$

■ a: stochastic term

- intrinsic statistical shower fluctuations
- sampling fluctuations
- signal quantum fluctuations (e.g. photo-electron statistics)

■ b: constant term

- inhomogeneities (hardware or calibration)
- imperfections in calorimeter construction (dimensional variations, etc.)
- non-linearity of readout electronics
- fluctuations in longitudinal energy containment (leakage can also be $\sim E^{-1/4}$)
- fluctuations in energy lost in dead material before or within the calorimeter

■ c: noise term

- readout electronic noise
- Radio-activity, pile-up fluctuations

Effects on energy resolution

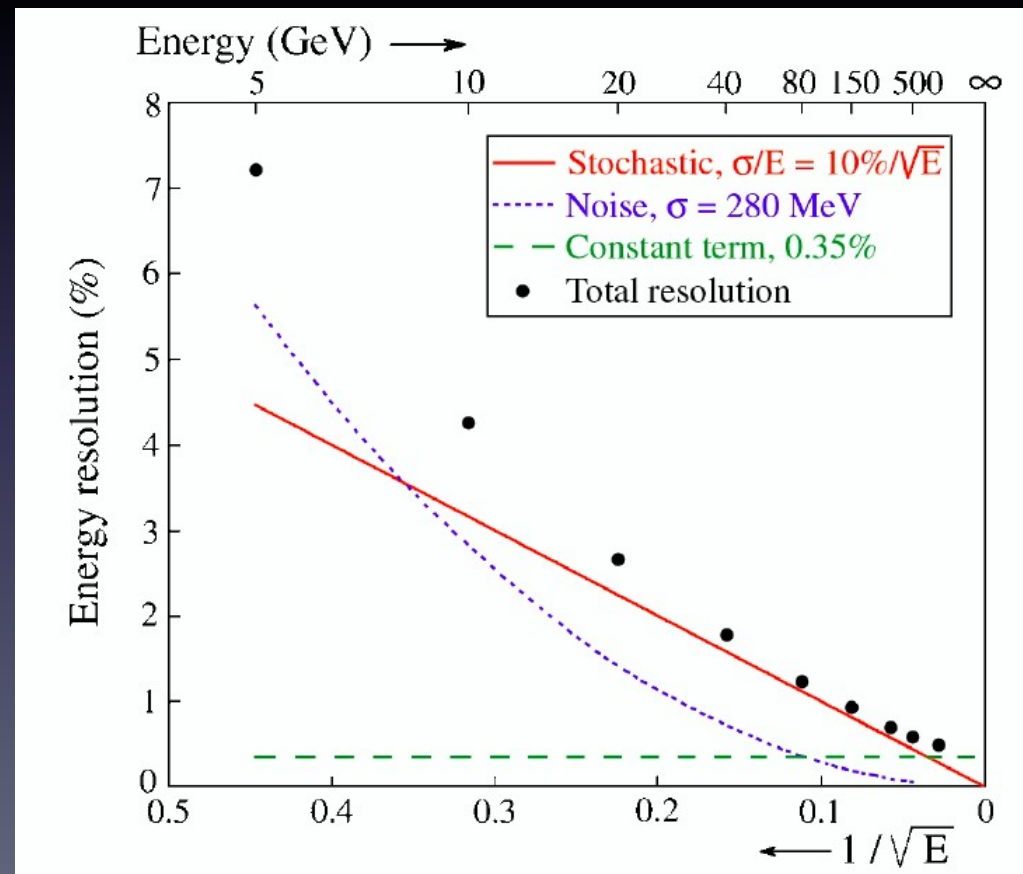
ATLAS EM calorimeter

Different effects have different energy dependence

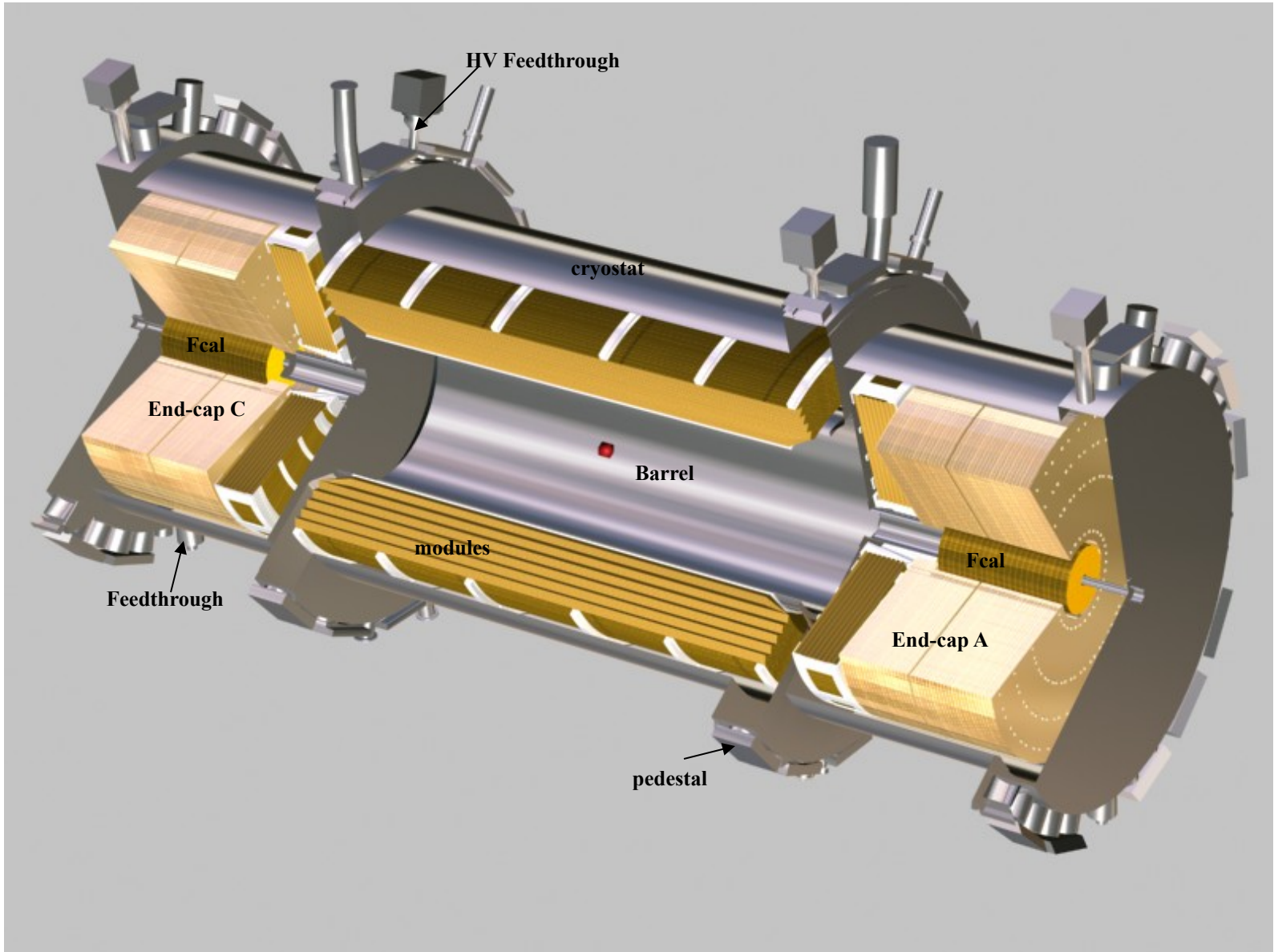
- Sampling fluctuations
 $\sigma/E \sim E^{-1/2}$
- shower leakage
 $\sigma/E \sim E^{-1/4}$
- electronic noise $\sigma/E \sim E^{-1}$
- structural non-uniformities:
 $\sigma/E = \text{constant}$

$$\sigma_{\text{tot}}^2 = \sigma_1^2 + \sigma_2^2 + \sigma_3^2 + \sigma_4^2 + \dots$$

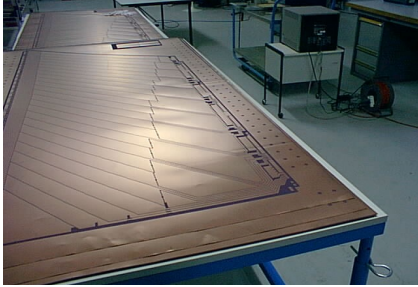
$$\frac{\sigma(E)}{E} = \frac{10\%}{\sqrt{E}} \oplus \frac{170\text{MeV}}{E} \oplus 0.7\%$$



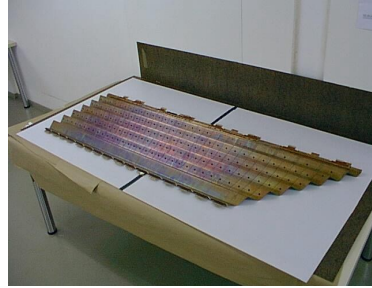
**Picture Book of US ATLAS
Liquid Argon Calorimeter
Construction**



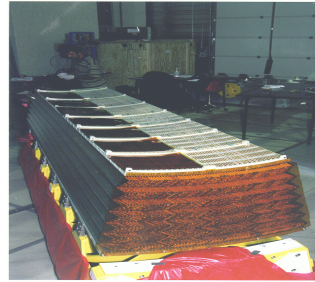
Electromagnetic module



Electrode



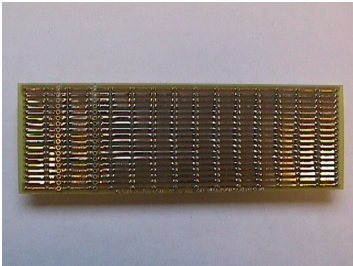
Electrode bending



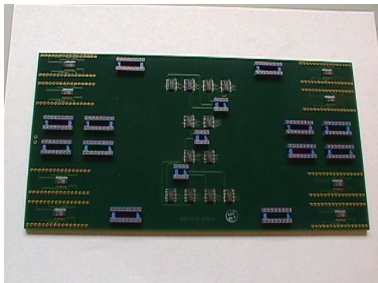
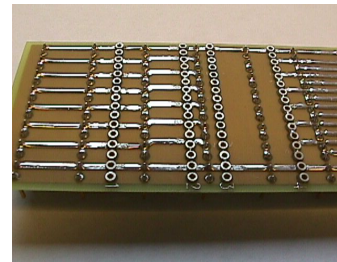
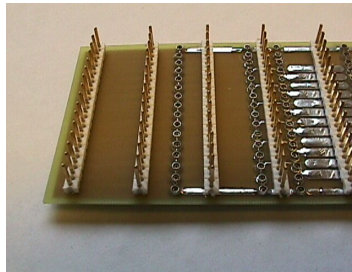
Module assembly



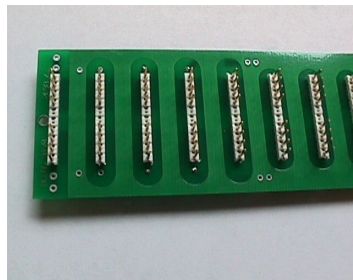
Completed module



Summing boards

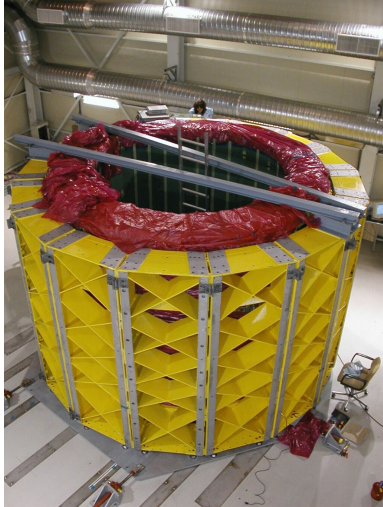


Mother boards

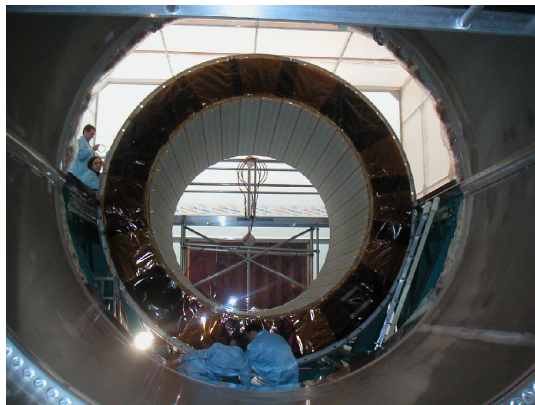
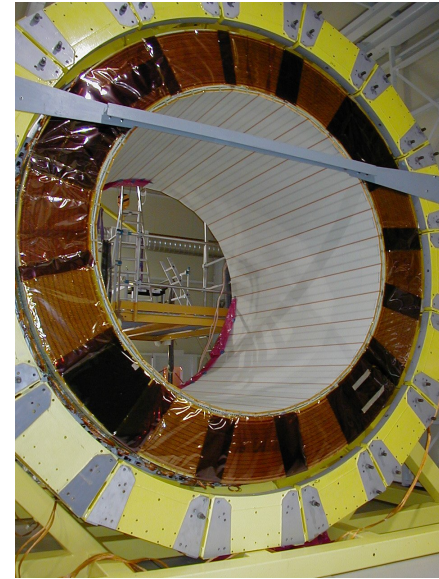


HV boards

Electromagnetic modules



**Half-barrel wheel assembly
16 modules**



**Installation into the
cryostat**

Cryostat



Construction



Feedthrough assembly



Testing



Transport

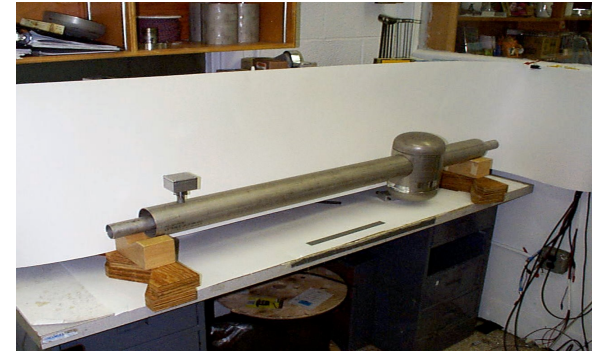


Integration

Cryogenics components

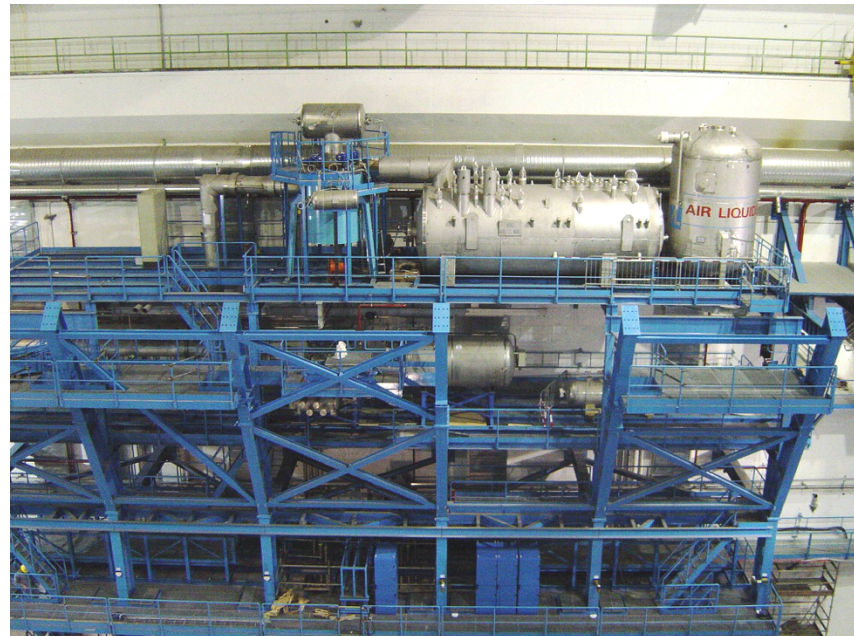


Separation Dewar



Quality meter

Proximity piping



Cryogenics in SH1

**Helium main
refrigerator
compressor
station**

**Helium shield
refrigerator
compressor
station**

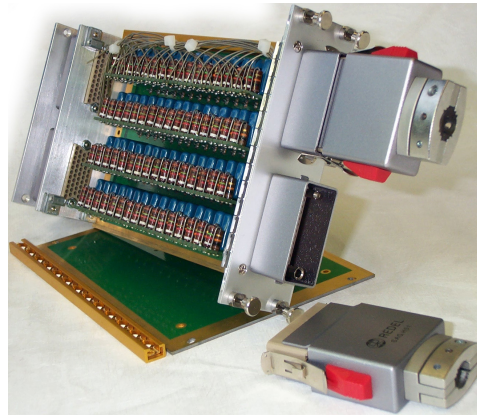


**Nitrogen
refrigerator
compressor
station**

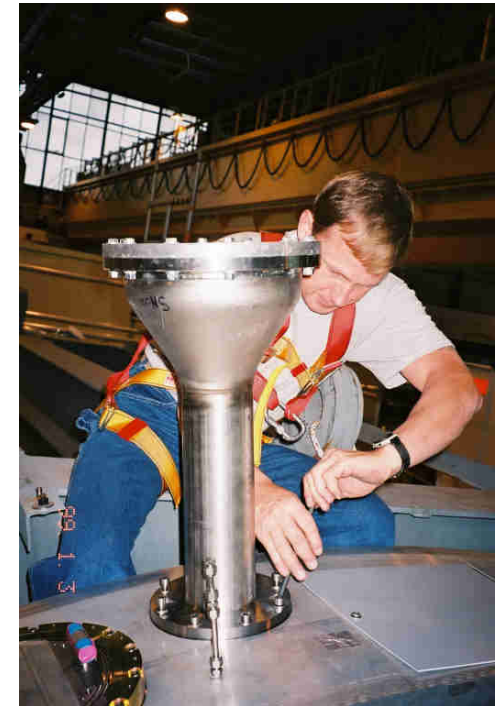
Feedthroughs



Signal Feedthrough



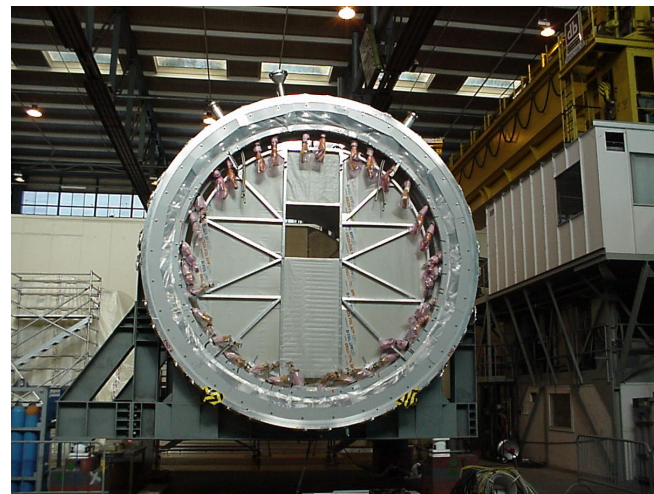
HV filter box



HV Feedthrough

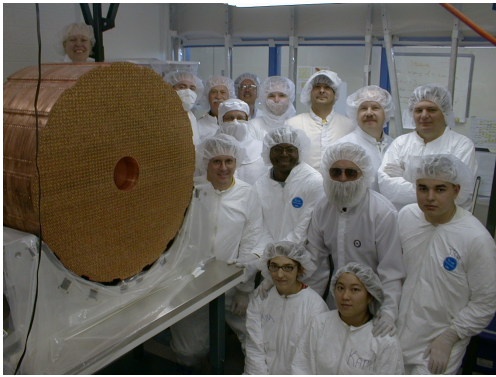


Signal Feedthrough –ready for installation



**Feedthrough's
installation completed**

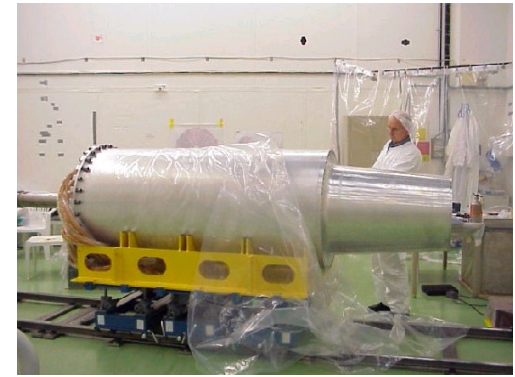
Forward Calorimeter



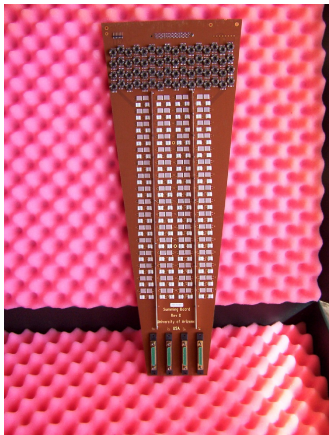
First module



Module assembly



Ready for installation



Summing board



Installation

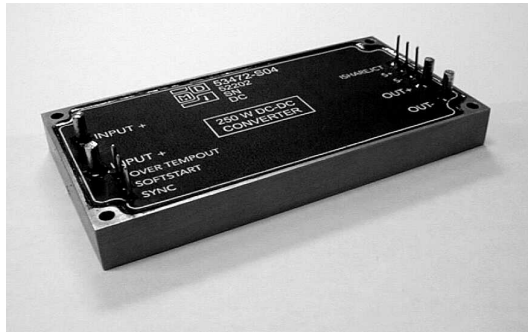


Electronics installation complete



Endcap assembly complete

Crates and Power supplies



DC-DC converter module



Power supply unit



**Power supply installed
on the barrel**

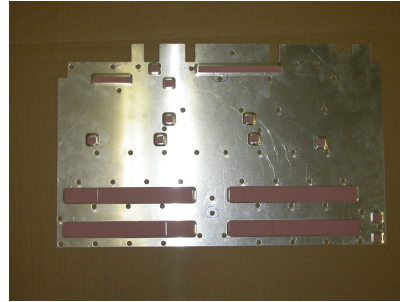
**Front End
crate**



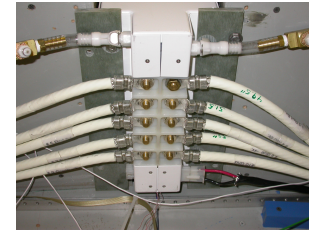
Cooling and services



Cooling plate



Heat transfer plate



Low voltage cables and connectors



Cooling pipes, cable trays and local cables



Cable trays for the calorimeters services

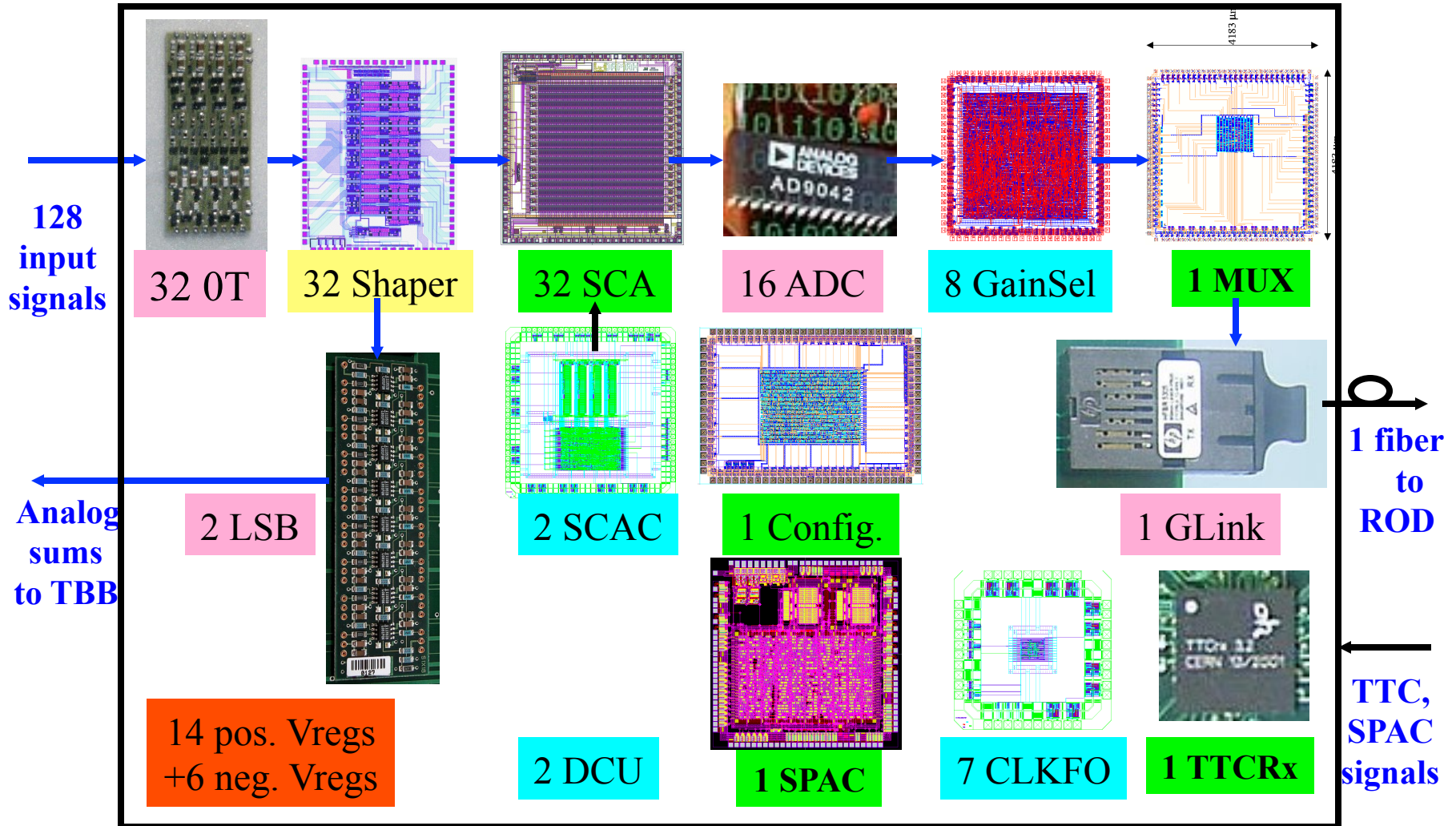
Front End Board

DMILL

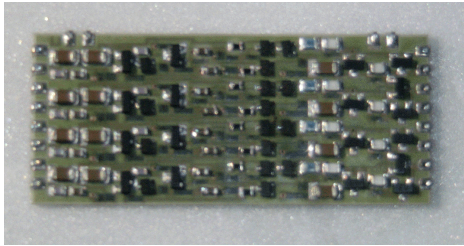
AMS

DSM

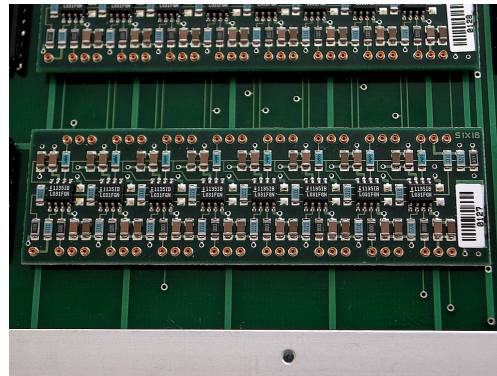
COTS



Readout electronics

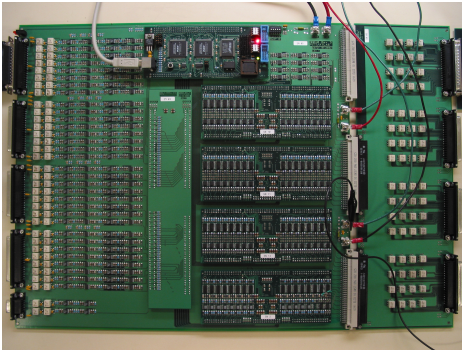


Preamplifiers

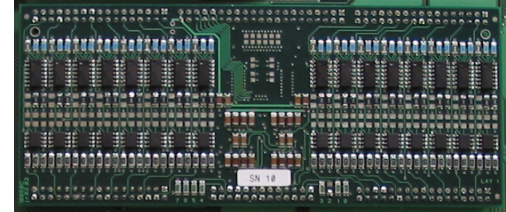


Layer sums board

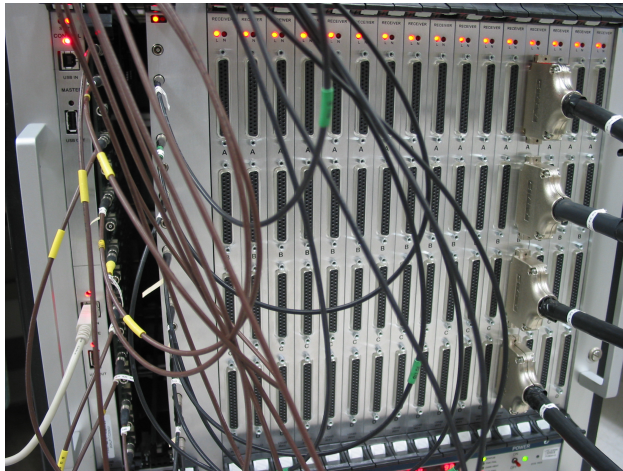
Level 1 Receiver



LV1 Receiver board



Variable Gain Amplifier



Front



Back